Sudan University of Science and Technology

College of Graduate Studies

Ablation of Molybdenum by Femtosecond Laser Pulse Using the Two-Temperature Model

إزالة الموليبدينوم بواسطة نبضة ليزر الفيمتو ثانية باستخدام نموذج درجتي الحرارة

A Thesis Submitted in Partial Fulfillment of the Requirements for Degree of M. Sc. in Physics

Prepared By:

Nafisa Mohammed ALkhader abdullah

Supervisor:

Dr. Isam Ahmed Attia

November 2020

الآية

يقول الله تعالى

﴿إِنَّا كُلَّ شَيْءٍ خَلَقْنَاهُ بِقَدَرٍ (49) وَمَآ أَمْرُنَآ إِلاَّ وَاحِدَةٌ كَلَمْحٍ بِالْبَصَرِ (50)﴾

سورة القمر

Dedication

To my angel in life.to the meaning of love and meaning of tenderness

To the smile of life and the mystery of existence

To my most beloved dear mother

To whom I proudly carry his name I ask God to extend his life to see fruits that are ripe to be harvested after a long wait

MY DEAR FATHER

To everyone who stood beside me and extended a helping, my brother, sisters and friends

Acknowledgement

The supreme of the verses of thanks and gratitude I dedicate to my supervisor who characterizes me beautiful style and upscale dealing **Dr.Issam Ahmed Attia** for the wok he presented to me and he did not spare me any information, as well as for the good treatment of me, you all thanks and appreciation

We thank all those who participated in this humble effort

Abstract

The study generally presents the mechanism of ablation of metals by ultrafast laser pulses; the main part was devoted to understanding a particularly interesting case: femtosecond pulse laser irradiation.

Femtosecond ablation heating is described by a two-temperature model based on the Fourier heat transfer equation. This model consists of two parabolic differential equations coupled by the exchange term between the two subsystems, namely the electron gas and the ion network.

The ultra-rapid heating mechanisms in metallic material have been studied by an approach based on numerical simulation, where the study of ultra-short pulse heating has been carried out on a Molybdenum slide.

The work carried out consists in the construction of a geometry representing the domain of computation, thanks to the Gambit preprocessor, then to solve the equations coupled by the Fluent processor. The results obtained concerning the distribution of the temperature field show conformity with those obtained by other authors.

The applications that can be envisaged with a laser with femtosecond pulses fired at a given frequency (a few MHz) open the way to nonmetric structuring which can be applied to advanced techniques for the exploitation of solar energy for example

المستخلص

تقدم الدراسة بشكل عام آلية استئصال المعادن بواسطة نبضات ليزر فائقة السرعة، وقد تم تخصيص الجزء الرئيسي لفهم حالة مثيرة للاهتمام بشكل خاص: تشعيع نبض الفيمتو ثانية.

يتم وصف تسخين الاجتثاث من الفيمتو ثانية بواسطة نموذج ثنائي الحرارة يعتمد على معادلة فورييه لانتقال الحرارة. يتكون هذا النموذج من معادلتين تفاضليتين مكافئتين مقترنين بمصطلح التبادل بين النظامين الفرعيين، وهما غاز الإلكترون وشبكة الأيونات.

تمت دراسة آليات التسخين فائقة السرعة في المواد المعدنية من خلال نهج قائم على المحاكاة العددية، حيث تم إجراء دراسة التسخين بالنبض شديد القصر على شريحة موليبدنوم.

يتكون العمل الذي تم تنفيذه من بناء هندسة تمثل مجال الحساب، وذلك بفضل معالج جامبيت ، ثم لحل المعادلات المقترنة بمعالج فلوينت. أظهرت النتائج التي تم الحصول عليها بخصوص توزيع مجال درجة الحرارة مطابقة مع تلك التي حصل عليها مؤلفون آخرون.

التطبيقات التي يمكن تصورها بالليزر مع نبضات الفيمتو ثانية التي تُطلق على تردد معين (بضعة ميغا هرتز) تفتح الطريق للهيكلة النانومترية التي يمكن تطبيقها على التقنيات المتقدمة لاستغلال الطاقة الشمسية على سبيل المثال.

Table of Contents

Chapter Three

Two Temperature Model of Laser Interaction Femtosecond with A metal

Chapter Four

Numerical Processing

Chapter Five
Conclusion & Future Work

List of Symbols /Abbreviations

Mo	Molybdenum
MoOx	X^{th}-Molybdenum Oxide
TTM	Two temperature model
N d YAG	Neodymium-doped yttrium Aluminum Garnet
LASER	Light Amplification by Stimulated Emission of Radiation
UDF	User defined function
VOF	Volume of Fluid
BI	Bremsstrahlung
CFD	Computational Fluid Dynamics
PPM	Part Per Million

List of Figures

List of tables

Table no.	Title	Page
4.1	The calculation parameters.	37

Chapter One

Introduction

1.1 Preface

The structuring of metal surfaces by laser is a technology that is developing rapidly given the enormous potential and possibilities offered by miniaturization for many applications.

Indeed, many material properties can be modified by acting on the surface topography, for example, the optical, tribological, adhesion, chemical, etc. characteristics can be controlled by adequately producing the surface structures to make them match the need for a specific application.

The ablation of matter by ultrashort laser pulses makes it possible to control these characteristics on a micrometric or even nanometric scale.

The effect of the propagation of heat under operating conditions, where electromagnetic energies delivered in an ultra-fast time are used, makes that the response to the absorption of the incident energy by the material is done in a completely different way compared to what is commonly encountered in conventional heating processes.

In an extremely short duration, of the order of a hundred femtoseconds (1fs = 10^{-15}s) the material sees the energy deposited over a length comparable to the thickness of optical penetration which is of the order of ten nanometers for several metals. It is considered on this timescale that the material treated is divided into two subsystems in the case of metals: the ionic network composing most of the material, and the electronic gas composed of free or bound electrons. On the time scales of a laser pulse lasting a few hundred femtoseconds, only the electrons respond to the electromagnetic stress and it is the electrons that absorb the laser energy while the ions in the network have no time to feel the electromagnetic shock and remain undisturbed. These are the electrons that redistribute in the network the energy gained well after the end of the laser pulse.

1.2 Statement of the Problem

In recent decades, Ultrashort pulse laser has found increasing applications in broad fields including material processing, chemistry, biology, health, medicine, electronic, and information technology. The ultrashort pulse duration, usually in the order of femtoseconds to hundreds of femtoseconds, presents its unique properties such as very high peak power, very limited thermal effects, compared with long pulse laser. The interaction mechanism between ultrashort pulse laser and materials is of importance due to its more and more broad applications. In the theories describing material changes after ultrashort laser pulse radiation, the two-temperature model (TTM) [1] is well-known and widely used. In this model, the absorption is divided into two processes. When ultrashort laser pulses arrive at the surface of a metal, the free electrons in the metal first absorb the energy of the laser light, that is, photons. Then there are two paths for the energy absorbed by the electrons to rearrange the thermal diffusion of the hot electrons and the collisions between the electrons and phonons. The latter interaction makes the material temperature rise. Based on this consideration, Anisimov et al [2].obtained the TTM.

1.3 Aims

The objectives of this project are as follows:
1. To focus on the laser-metal interaction in femtosecond regime.
2. To this end, our study is developed around the two-temperature model, in which the absorption of laser radiation by the electron gas is taken into account first, then the energy transfer from the electrons to the ion network .
3. Constituting the main material, where the thermal effects will appear.
4. The study will focus on the interaction of a laser delivering ultra-short femtosecond pulses with Molybdenum.

1.4 Methodology

Many physical phenomena can be modelled by differential equations, but -apart from some very specific cases – it is generally not possible to write down the solution to these problems in closed form. In order to understand the behavior of the solution, it is thus often necessary to construct an approximation via a numerical solution.

Our research concerns on a numerical simulation, to describe the evolution the interaction of a laser delivering ultra-short femtosecond pulses with Molybdenum

1.5 Questions

How the Nd–YAG pulsed laser irradiation on metals in air ambient?
How the thin films of molybdenum (Mo) interacted which irradiated by a femtosecond laser source?
How the structure of their surfaces and control the oxidation valence of the photo induced MoO_x surface layer.

1.6 Thesis Lay Out

The thesis is made up of five chapters, where it will give in the e first chapter introduction, the second chapter generalities on molybdenum and on pulsed lasers, then an overview on laser ablation and laser-metal interaction.

The Third chapter is devoted to the presentation of the two-temperature model, where the foundations will be exposed, then it will talk about the absorption of laser energy and relaxation. it will develop femtosecond laser ablation, and the resulting effects, especially for surface modification. will present at the end of the chapter the model to be solved with the most important physical parameters, including the source term and the electron-phonon coupling constant.

In the Fourth chapter, the application of the two-temperature model will be implemented for the study of the interaction of a pulsed Nd-YAG laser, whose pulse duration is 290 fs, with a metallic material which is the molybdenum. It will first present the calculation code used, consisting of the Gambit Preprocessor, the Fluent processor, the UDF procedures developed, and the Volume Of Fluid (VOF) interface monitoring method used in our digital modeling by the finite volume method. . It will give in this chapter the results showing the evolution of the temperature field during the absorption of the energy of the laser pulse by the electron gas, then that of the evolution of the temperature field during relaxation by redistribution of l energy to the metal ions of the network. In the chapter conclude the thesis.

Chapter Two
Interaction of Lasers with Metals

2.1 Introduction

The use of laser radiation as a source of vaporization of materials was first applied in the 1970s. Since then, the field of laser-matter interaction has grown much more over the past forty years; until becoming today a full-fledged branch of physics. Among the pioneers who contributed to the study of laser-matter interaction, its already found in the 1970s a model proposed by Ready [1], then taken up again by Von Allmen in 1976 [2].

Before going into the description of the laser-matter interaction process, it is useful to speak briefly in this chapter above the material which constitutes the part of treated in this study, and the source of radiation which interested, which is the laser. Femtosecond, where will discussed the operating principle.In the second part of this chapter, will give a brief introduction to the basic principles that govern the propagation and absorption of laser radiation, as well as the response of the irradiated material.

2.2 General

2.2.1 Notions on Molybdenum

Long considered a rare element, where its abundance in the earth's crust is 1.2 ppm, Molybdenum is a transition metal with symbol Mo, atomic number 42, and atomic mass 95.94. It is located in the fifth period in group VIB of the Mendeleev periodic table; it is silvery white in color and has a centered cubic crystal structure [3]. In nature, it is found in ores (molybdenite, powellite and wulfenite), volcanic rocks, limestones, etc.

| Wulfenite | Powellite | Molybdenite | Molybdenum |
| ($PbMoO_4$) | ($CaMoO4$) | (MoS_2) | |
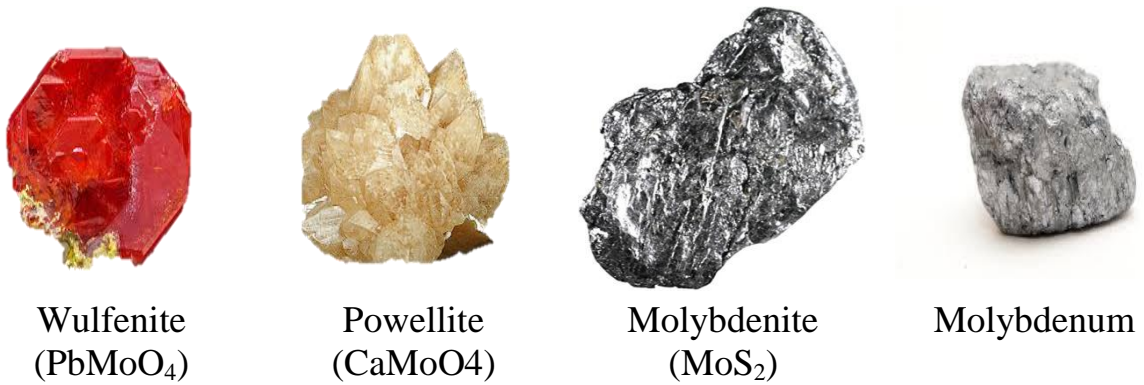
Figure 2.1: Molybdenum in its natural state.

It was discovered in 1778 when Carl Wilhelm Scheele caused the separation of the components of Molybdenum from those of graphite and lead, which have always been confused; hence its non-Greek "molybdos" which means "resembles lead". However, it is valued as an exceptional material which can meet even the most requirements. Indeed, to these mechanical and thermal properties:

- Refractory, malleable, and hard materials,

- A very high melting point 2625°C,

- A boiling point at 4639°C,

- A low coefficient of expansion,

- High thermal conductivity (138 $W.m^{-1}. K^{-1}$),

- a high modulus of elasticity,

- Excellent resistance to corrosion.

Because these alloys are used for different uses including energy or transport infrastructure such as automotive, air, substrates for hot surface deposits...etc [3].

2.2.2 Ultra-short laser pulse

▢ Lasers

The letters L.A.S.E.R constitute the English acronym for Light Amplification by Stimulated Emission of Radiation, which has the meaning: Amplification of Light by Stimulated Emission of Radiation [4]. The laser is a major invention of the twentieth century, which occurred in the early sixties. The first laser emission was obtained by Théodore Maiman using a ruby crystal as an active medium or an amplifier.

Basically, a laser device consists of an amplifying medium placed between two mirrors, of identical axis, the whole of which constitutes what is called a resonant cavity. A light source provided for example by flash lamps causes the emission stimulated by back and forth in the cavity causing, passing through the amplifying medium, the generation of a large number of photons of the same wavelength , which will be amplified and will give rise to an electromagnetic, monochromatic wave, spatially and temporally coherent. Also, the resulting electromagnetic wave is essentially characterized by its directionality, which constitutes the particularity of the laser beam [4].
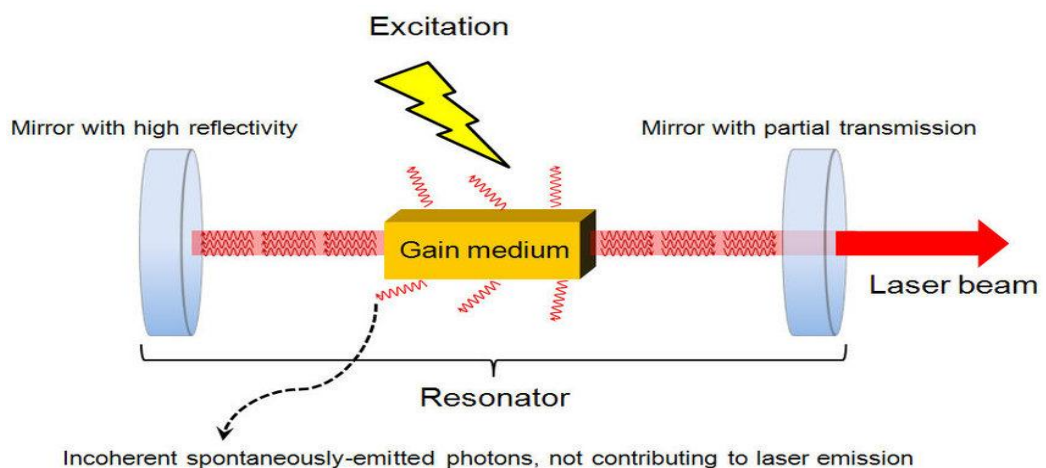
Figure 2.2: Principle of operation of a laser.

It can separate the different types of lasers in relation to their operating modes continuous or impulse. Depending on the nature of the amplifying medium, it can cite:

6

- Solid-state lasers (ruby laser, Nd-YAG),

- Gas lasers (helium-neon laser, ionized argon laser),

- dye lasers,

- Excimer lasers

- Chemical lasers.

- Semiconductor lasers

Among these lasers, a very specific class produces extremely short pulses, called ultra-short lasers.

☐ Ultra-short laser

Ultra-short pulses result from the modification of the properties and constituents of ordinary laser systems [5], The term ultra-short, or ultra-brief, or even ultra-fast generally indicates the range of pulse duration when 'it extends from the picosecond (10^{-12}s) [6], to a few hundred femtoseconds (10^{-15}s). Furthermore, the implementation of attosecond pulses (10^{-18}s) has already been demonstrated in the laboratory [5].

☐ Generation of a femtosecond laser pulse

Obtaining a short duration, high power pulse requires two steps: producing short pulses; then amplify them. A femtosecond laser beam has an amplifier emitting in a very wide band of the order of

a few hundred nanometers, with a mode blocking mechanism, and dispersion compensation. As is well known, in an "ordinary" laser cavity, several modes of random phases and irregular amplitudes can propagate: these modes being combined produce laser radiation. Thus by the mode-locking process11 (mode-locking), these different modes will be brought into phase at a well-defined instant, this results in a train of extremely fine pulses; in fact, the superposition of several harmonics of phases, of regularly spaced frequencies, gives rise to a train of pulses that is all the more finer and more intense than there are modes

(Figure 2.3). Thereafter, unwanted noise is eliminated between two successive peaks [6]. Thus, one can amplify only the short pulses, and it is these which are emitted: it is the locking of the modes [7].
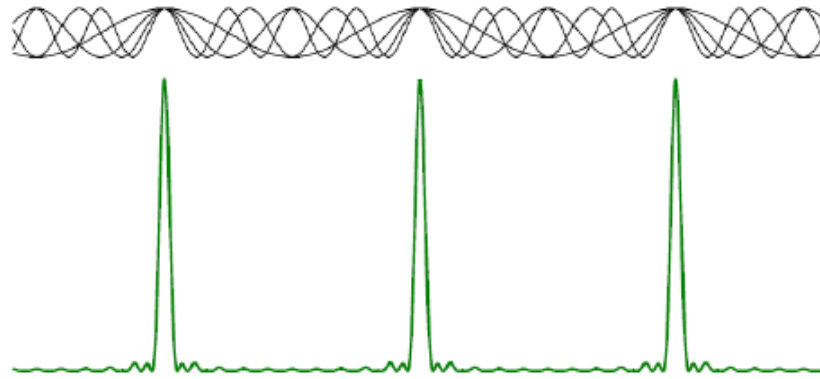
Figure 2.3: Example for eight modes in phase [6].

2.3 Laser ablation of a metal target

2.3.1 Interaction of a laser with a solid

Laser ablation is a technique of removing material from a substrate by a laser beam without damaging the structure of the material. This mechanism is of great interest due to its many uses. Indeed, the specific interactions of laser light with a material can lead to permanent changes in the properties of the material, which cannot be easily obtained by other methods [8].

The principle of the laser-matter interaction process is to concentrate a laser beam of given power on a target, where the absorbed light energy will then be converted into thermal energy on the surface of the material. This gives a restricted area of the target which will be subjected to heating, which can lead to the very localized fusion of a thin layer of the solid, once the latter reaches the ablation threshold. For metals, this threshold is included for fluency's between 1 and 10 J/cm^2, for insulators it is located between 0.5 and 2 J/cm^2, and for organic materials it is between 0.1 and 1 J/cm^2 [8]. During laser ablation, the material vaporizes almost instantaneously (Fig 2.4).Can be observing the

formation of plasma which results from the interaction of the evaporated matter with the laser beam, and subsequently its expansion in the ambient medium [1]. This mechanism differs according to the characteristics of the laser beam, namely: the fluency, the wavelength, the duration, and the power of the pulse as well as the impact diameter of the beam on the target.
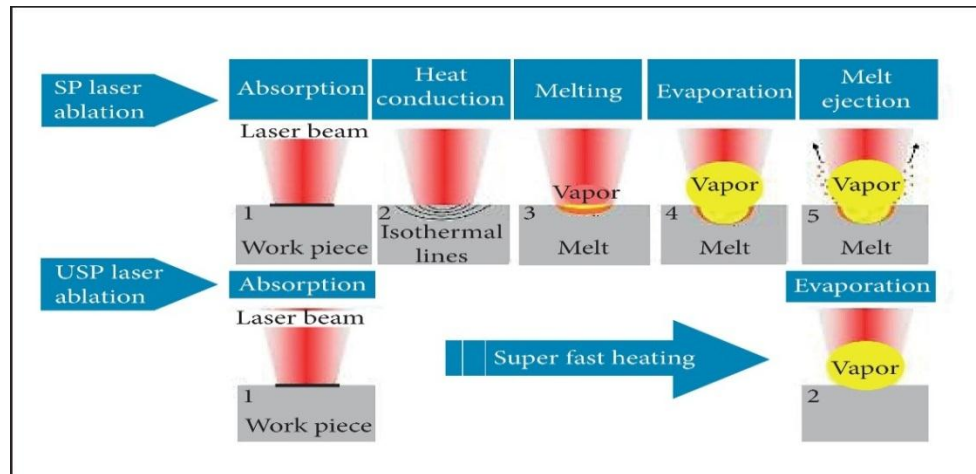
Figure 2.4: Mechanism of the laser-matter interaction.

Absorption, heating, melting, vaporization, the "piston" effect, plasma formation, Marangoni convection, and Kevin-Helmholtz instability are some aspects of the laser-matter interaction [9] which can induce modifications of local chemistry, local crystal structure and local morphology [8].

Since the phenomena involved in the interaction of laser radiation are complex and varied, it is extremely difficult to include them in a single study. By introduce them in all of the following in terms of energy absorbed and heat transfer, which are the essential mechanisms governing the laser-matter interaction.

The basic processes of absorption of radiation by matter are the same in all types of materials. However, what makes their behavior different is the predominance of some of these processes over others [6]. For example, in dielectrics and semiconductors, where the density of free electrons is very low, a complex absorption mechanism is governed by the predominant phenomenon of resonance excitation. This allows the creation of free carriers, following

ionization. Thus, the laser energy is absorbed by the free electrons due to the reverse Bremsstrahlung absorption mechanism. Also, another significant part will be absorbed by the states located in the gap (faults and impurities) [10,9]. When it comes to metals, the process is practically different.

☐ **Structure of a metal**

A metal is a crystalline solid made up of two subsystems: a quasi-fixed ion network forming a localized periodic structure, and a gas of weakly bound free electrons, exhibiting an ultra-fast dynamic response accessible to excitations in the optical and infrared [11].

☐ **Thermal effect**

In metals, the potential energy level of the free electrons of the metal is in the conduction band. During its irradiation, the electrical component of the electromagnetic wave causes the oscillation of free electrons and their collision in the conduction band; this means that the energy carried by the radiation is directly transmitted to the very dense electron cloud. free. Thus, for most metals, a large part of the energy absorbed is converted into thermal energy by the electron-phonon interaction in a time of the order of 10^{-10} to 10^{-12} s, which corresponds to durations shorter than the duration of a laser pulse in the nanosecond. Such processes are characterized by the photo thermal mechanism [8].

The nature of the ablation also depends on the type of metal. Indeed, the energy density at the ablation threshold depends on the cohesion energy of a metal, but also on its thermal conductivity. In fact, the lowest values are obtained for metals whose energies are less than 3 eV per atom such as Cd and Pb, transition metals (Ni, Fe, Co) as well as noble metals (Ag, Au) have intermediate threshold energies and finally the refractory metals (W, Ta, Mo) have maximum threshold energy densities (greater than 6 eV per atom) because they have the highest binding energies. In addition, once the ablation threshold has been reached, increasing the energy density only overheats the ablated region [6], this explains

why the volume of the area affected thermally during irradiation is limited.

☐Equation of heat

The irradiation of a material in general and of a metal in particular by a laser beam is accompanied by an energy transfer and a heat flow described by the heat transfer equation. The latter defines the spatial and temporal evolution of the temperature field in the solid.

In 1807, Jean Baptiste Joseph Fourier proposed a law valid in all points of a volume which links the density of the flux φ (Wm^{-2}) to the thermal conductivity k (Wm^{-1}K^{-1}) and to the local gradient of the temperature field T (x, y, z, t) [12]:

$$\vec{\varphi} = -k.\vec{\nabla}T \qquad (2.1)$$

The presence of the sign (-) in the formulation means that the heat flow opposes the temperature gradient and that it only exists in the presence of this gradient. On the basis of this law, Fourier established a parabolic partial differential equation, which governs heat transfers in variable temperature regime, and thus resulted in the general heat transfer equation [13] given by:

$$\rho c_p \frac{\partial T}{\partial t} = \vec{\nabla}(k.\vec{\nabla}T) + S \qquad (2.2)$$

Where ρc_p is the specific volume heat of the material, and S is a heat source which in our case can be compared to the effect of a laser beam. This equation reflects the fact that the temporal variation of the temperature in the material is only the exchange of heat by convection on the surface added to the creation of heat.

2.3.2 Response of a metal to laser irradiation of different pulse durations

Despite the influence of energy and various parameters, the reaction of a metal to a laser beam depends essentially on the pulse duration of the latter. The comparison of the continuous, nanosecond, picosecond and femtosecond pulse regimes is focused on the two thermal and dynamic aspects of the interaction of the laser with matter:

From a thermal point of view, the impact of the laser beam on the material is no longer the same for the different pulse regimes mentioned above (Fig 2.5).
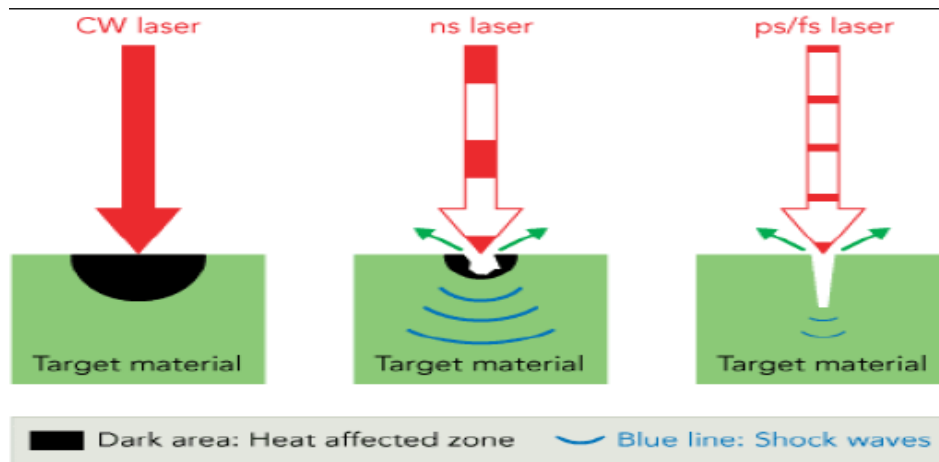
Figure 2.5: Basic phenomena of the irradiation of a material at different durations of action of the laser [14].

For a given incident laser energy, the longer the pulse duration, the lower the temperature reached; and the greater the heated depth, if the energy contained in the beam is sufficient to cause vaporization; the vaporized thickness increases with the pulse duration, on the other hand if the energy is insufficient to maintain the vaporization, it will be lost by conduction inside the treated material. Conduction losses are all the more important as the medium is a good conductor. Conversely, if the pulse duration is small, the temperature reached by the surface is important and the heated depth is reduced [15].

Following studies carried out on the scale of a sub picosecond pulse ($<10^{-12}$s); and of a nanosecond pulse (10^{-9}s), It realize the difference in the behavior of the two extreme cases of short and long pulse, where the result is illustrated qualitatively in the figure below [16]:
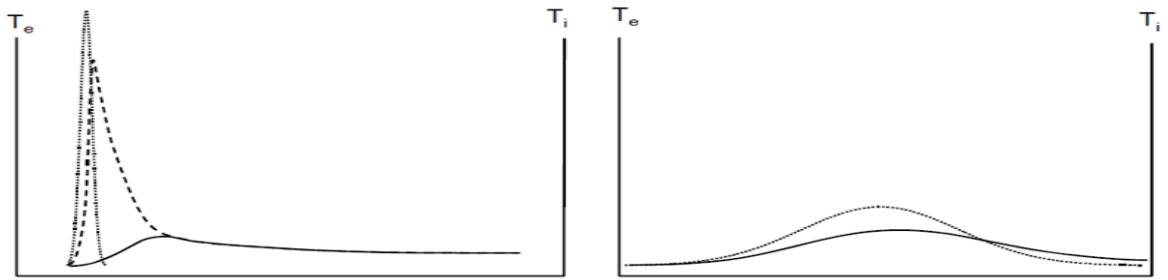
Figure 2.6: Evolution of the thermal field for a material subjected (on the left) to an ultrashort impulse (on the right) to a long impulse. Dotted line: laser pulse, dashes: electronic temperature, solid lines: network temperature.

For the ultra-short pulse, it first observes an electronic heating phase; followed by cooling of the electrons while the temperature of the network increases. In the case of the long pulse, the electronic temperature and the network temperature change simultaneously.

From a dynamic point of view, if the radiation intensity is sufficient, a part of the metal is ejected in the form of plasma, ions and aggregates, a crater is formed on the surface of the target with a depth and a geometry which depends on the shape of the beam [6] (fig 2.7 a, b). In the figure it note the difference between the holes drilled in a thick metal sheet (in a vacuum) with laser pulses with two different pulse regimes: femtosecond and nanosecond.
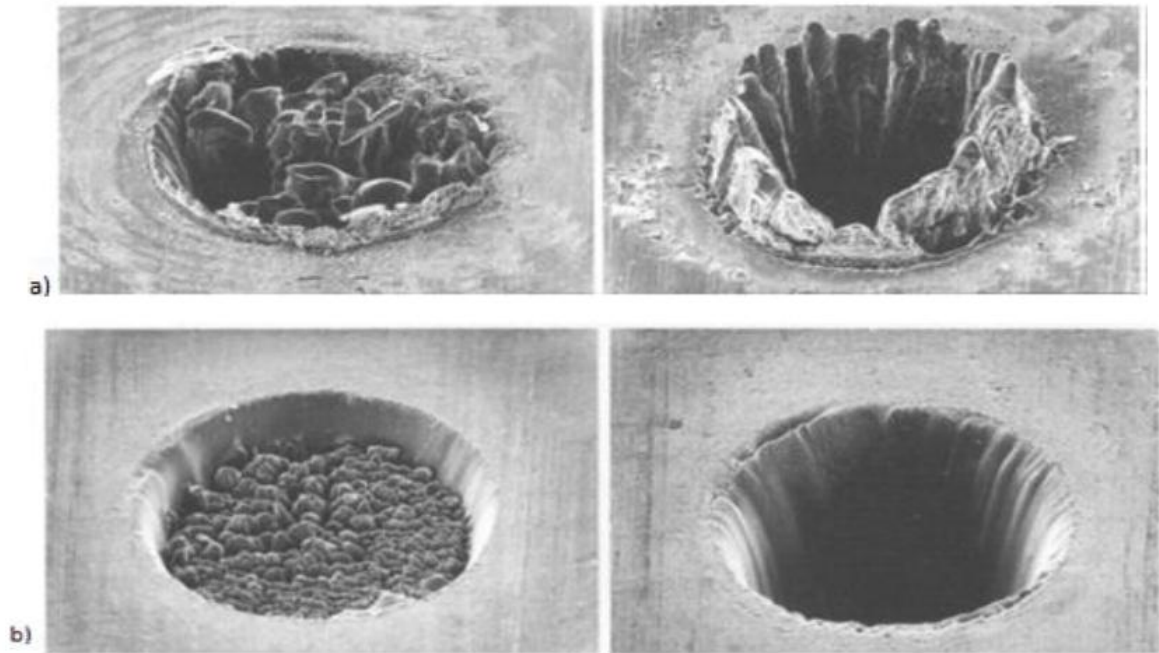
**Figure 2.7: Holes drilled by laser ablation with a) a second pulse,
b) a second pulse [17].**

In the case of ablation with nanosecond pulses (Fig 2.7a), the thermal wave has enough time to propagate in the metallic material and produce a relatively large fusion, where the presence of a liquid phase leads to an unstable drilling process. In this case, the target material is removed both in a vapor phase and in a liquid phase; the vaporization process produces a recoil pressure which expels the liquid. On the other hand, in the case of the femtosecond pulse (Fig 2.7b), there is no trace of the molten material; a clean, burr-free ring is obtained.

2.3.3 Advantage of femtosecond lasers in the treatment of materials

The use of ultra-short pulse lasers in the field of materials processing has been the subject of much growing interest in recent years, thanks to its advantageous characteristics compared to other lasers. It cite for example the fact:

☐ That they favor intrinsic processes over processes resulting from the presence of faults, especially in insulating materials. This is due to the fact that It can

work at higher radiations without reaching the threshold of breakdown of the material [16].

☐ Let the femtosecond laser directly vaporize the material, which gives a clean and precise result [7].

☐ That irradiation with an ultra-short pulse makes it possible to separate the phase of the laser-matter interaction from the phase of thermodynamic expansion. This allows us to confirm that in this case It are purely in a laser-solid interaction [16].

☐ That the use of a femtosecond pulse can give rise to a situation of notable thermal imbalance between the electrons of the material and the network.

Chapter Three
Two Temperatures Model of Laser Interaction
Femtosecond with A metal

3.1 Introduction

In the field of irradiation of materials with sub picosecond pulses, a specific treatment is necessary due to the invalidity of the laws of heat transfer at a single temperature. This type of laser-matter interaction is described by a purely thermal approach on the macroscopic scale by a model known as the Two temperature model' (TTM).

Long before the advent of lasers and their use in applications, the first version of a two-temperature model was proposed by Kaganov in 1957 [18]. Later, an interest in this model reappeared in the 1970s [19]. Thus, following research on evaporation due to absorption of short pulses by a solid, Anisimov proposed in 1974, a phenomenological parabolic model at two temperatures, to describe the transition between an out of equilibrium electron gas and the network [20]. Subsequently, a two-temperature hyperbolic model based on the Boltzmann transport equation was rigorously developed by Qiu and Tien in 1993 [21]. Such a model can be perfectly simplified into a parabolic model as proposed by Anisimov.

The TTM model describes the heating of the electron gas [18], and the exchange of energy between the electrons and the network, insofar as the two subsystems are supposed to be in thermodynamic equilibrium at different temperatures [22]. So, this consists in assigning a temperature to the free electrons and to the ionic network to define the spatial and temporal distribution of the temperature field within the metal in this ultra-short pulse regime.

In this chapter, It will try to understand first the basis of the TTM model, then It will be interested in some fundamental aspects of the femtosecond-metal laser

interaction, this in order to try to identify the potential advantages specific to the use of this pulse regime. Finally, it presents the system of equations describing the spatial and temporal evolution of the two temperatures in the material.

3.2 Foundation of the TTM Model

In order to better assimilate the causes which led to the need to propose the TTM model to treat ablation with an ultra-short laser, It will focus on two important effects, namely: the photon absorption mechanism by electrons and to relaxation, in this pulse regime.

3.2.1 Phenomena of Absorption

When a femtosecond laser pulse is incident on the surface of a metal, the electrons are the first to react [23], and therefore it will first describe how electromagnetic energy can be absorbed by them electrons.

In a metal, the electronic density $n\ (E)$ is expressed as a function of the energy E by the Fermi-Dirac distribution [24]. According to the Pauli Exclusion Principle, when a photon of hν energy interacts with a metal, only electrons with energy between E_F and $E_F - hν$ will absorb the energy of the photons, then will be those between E_F - hν and E_F - 2hν.

Consequently, the absorption of several photons incites the release of more and more energetic states, thus leading to an electronic density distribution as shown in fig (3.1) [25]:
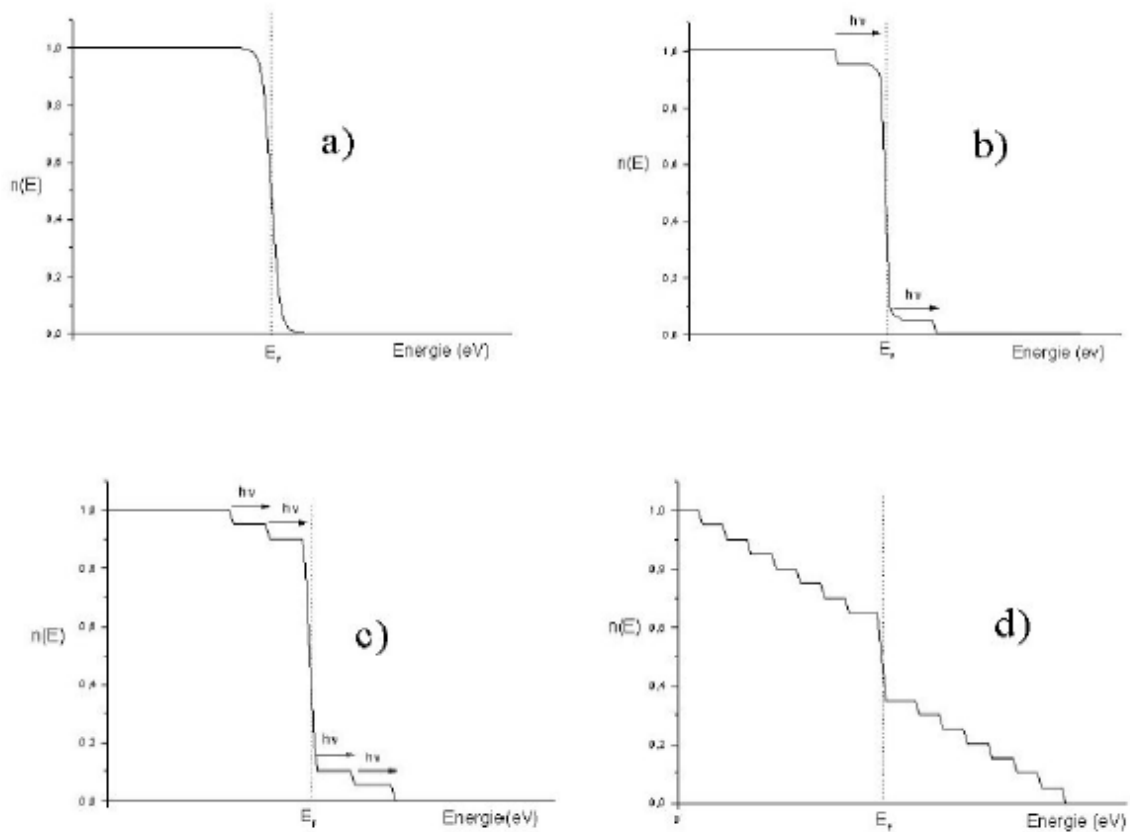
Figure 3.1: Density of electronic state as a function of energy. a) thermal equilibrium: distribution of Fermi-Dirac. b) initial absorption: the system is out of balance. c) release of the states E_F - hv, and possibility of absorption by the electrons of energy E_F -2hv. d) electronic distribution takes the form of a staircase.

In the presence of free electrons, this absorption mechanism occurs through the reverse Bremsstrahlung (BI) process [10, 17, 26], where the free electron can exchange energy with an external electromagnetic field. So, the electron goes to levels higher energies by gaining acceleration. It has been shown that absorption by BI is more effective in the vicinity of the critical density, which is on average equal to $3 \times 10^{-27} m^{-3}$ for metals [6]. It is ten times smaller than the electron density, and it is for this reason that the optical depth in metals is very low (around ten nanometers) [24]. In addition, if the energy of the photons is insufficient, the electron absorbs several photons at the same time by the phenomena of multiphotonic and two-photon absorption:

18

Multiphotonic absorption

It is defined by the atomic transition during which an atom simultaneously absorbs several photons via a virtual state [27] (fig 3.2). It is a nonlinear process [28], which occurs when the energy of a disturbed atomic state coincides with the energy of an integer number of photons, so as to satisfy the relation [29]:

$$E_a - E_b = k.h\nu \qquad (3.2)$$

E_a and E_b are the energies of the atomic levels considered, hν the energy of a photon, and k an integer.
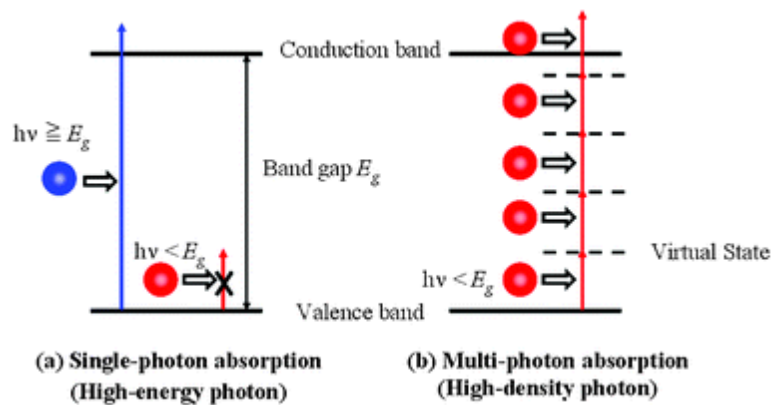
Figure 3.2: Representative diagram of electronic excitations in materials. a) Absorption of a photon. b) multiphotonic absorption [28].

The extremely high density of photons necessary to induce multiphotonic absorption can be easily generated by a femtosecond laser thanks to its power and its spectral finesse.

 Two photon absorption

In this case, the electron absorbs two photons almost at the same time, to achieve an existing state which corresponds to the sum of the energy of the incident photons. In order to reach a final state, no intermediate state is necessary, it rather consider a virtual state which does not correspond to a proper state of electronic or vibrational energy [30].

3.2.2 Phenomena of relaxation

The electron having acquired an energy carried by the electromagnetic wave of the ultra-short laser pulse finds itself disturbed and passes to a thermodynamic out-of-equilibrium situation, which will lead it to redistribute its energy by a process of relaxation.

Relaxation can be distinguished in three processes:

- The radiative processes,

- Collision processes (also called thermal processes),

- The trapping processes (which will not be mentioned in this manuscript).

◻ **Radiative relaxations**

These relaxations involve electron-hole recombination's; they are mainly encountered in semiconductors and occur less in the case of metals and dielectrics. In the study of interactions in femtosecond pulse regimes, these processes are not considered [6].

◻ **Relaxation by electron-electron collisions**

An excited electron interacts with all the other electrons in the system during which it transmits some or all of its energy to them. In the case of metals, this problem is dealt with by the so-called "Fermi liquid" theory 5 [6], these optically disturbed electrons have an out of equilibrium electronic distribution involving thermalization within the electrons [25] 6. In other words, the time for equilibrium of the temperature of the electrons is of the order of the inverse magnitude of the frequency of the electronic plasma, namely [10]:

$$\frac{1}{w_{pe}} \approx 10^{-2} fs \tag{3.2}$$

Studies have shown that the relaxation time of electrons can be reduced to 10^{-16} s at electron gas temperatures of 10^5 K [27]. The end of this step results in a Fermi-Dirac distribution, and therefore a temperature can then be associated

with the electrons. Thermal diffusion within the electron gas can then be started [25]. This type of collision is favored since the electron density is relatively high.

It is only after thermalization of the electrons that the thermal process of electron-phonon collision occurs.

☐ Relaxation by electron-phonon collisions

The electrons are also in interaction with the ions, and in this case, there is transfer of energy to the network of ions. In the context of the Born-Oppenheimer8 approximation, It consider that the displacement of ions around their equilibrium position is very low, which makes it possible to introduce the concept of electron-phonon interaction [25].

In the time preceding the thermalization of electrons, the electron gas and metallic network subsystems interact weakly [27], and thus, the transfer of energy from electrons to ions is much longer than the duration of the laser pulse (fig 3.3).

Indeed, in some numerical analyzes it has been found that the typical time for electrons and phonons to reach thermal equilibrium is a few picoseconds [22]. Consequently, conventional heat diffusion in the metal network cannot occur during the laser pulse.
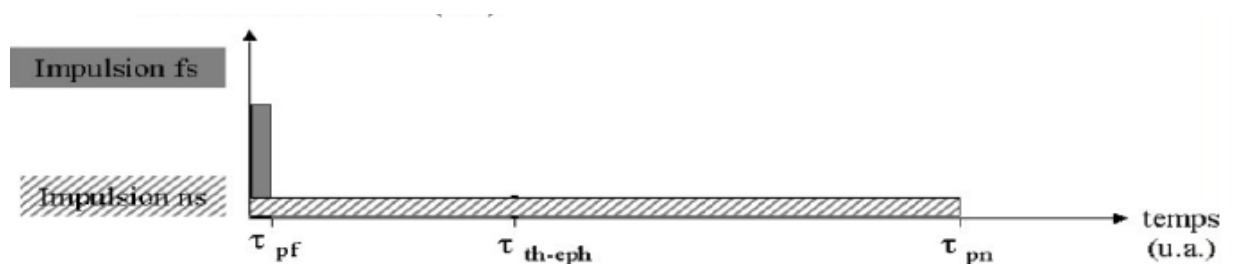

Figure 3.3: Comparative schematic representation of the femtosecond pulse duration with the characteristic time of the heat transfer to the phonons [25].

3.3 Irradiation process

3.3.1 Femtosecond laser ablation

The transfer of heat and energy in a metal optically excited by an ultra-short laser pulse takes place in three distinct phases (sketched in figure 3.4 [31]), namely [32]:

- Absorption of laser energy by electrons.

- Transport of energy by electrons and its relaxation.

- Thermal diffusion and thermodynamic balance of the target.

In the first step, the free electrons absorb the energy of the laser by electron-photon coupling during the pulse duration (fig 3.4a), this causes a thermal imbalance in the electron gas [33] and a rapid increase in the temperature of the latter [24]. The concentration of electrons absorbing the radiation

incident can be assessed by [27]:

$$n = \frac{h\nu N}{E_F} \tag{3.3}$$

Which ν the frequency of the incident light.

In the second step, there is first thermalization of the-e electrons, and once they have reached thermal equilibrium, the density of state can be represented by a Fermi-Dirac distribution, and at this instant- there, a temperature T_e can be attributed to electrons. At this stage, the temperature of the network remains that of the ambient [32, 34].

In addition, another competing phenomenon occurs, namely that the hot electrons diffuse in ballistic depth, and transport heat by ballistic movement; at a speed close to that of Fermi (10^6 m / s) [20,31].

Thereafter, a second phase begins, it takes place at t = th_{e-e}, where the electrons initially located in the ballistic range, will be pushed by the temperature gradient, and will diffuse in the deep part of the target (fig 3. 4b) [31]. They will thus transmit for a period of the order of a few picoseconds, their energy in the

network through the electron-phonon coupling [35], at a speed much slower than ballistic movement (10^4 m / s) [34].

The final phase begins at t = th$_{e-ph}$, that is to say when the electrons and the ionic network reach thermodynamic equilibrium, and this is how classical thermal diffusion takes place, and leads to the dissipation of heat in the mass [32] (fig 3.4c).
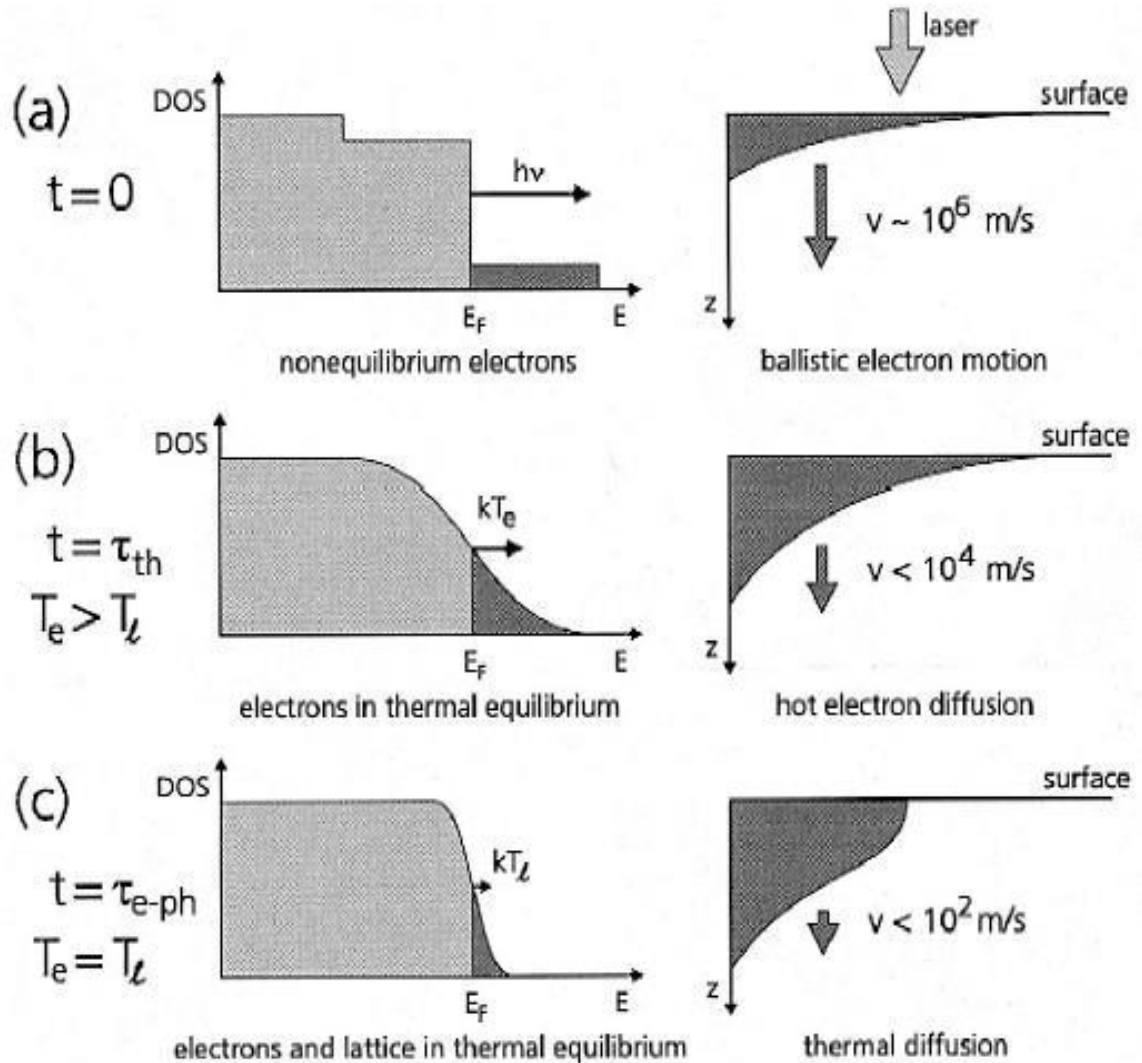

Figure 3.4: Three distinct phases of heat transfer in an optically excited metal.

3.3.2 Non-thermal effect

Observed by pump-probe studies, where non-thermal network fusion designates the loss of particles before 1ps, that is to say, before the material reaches a common temperature [23]. Indeed, overheating due to irradiation by ultrashort laser pulses is characterized by homogeneous nucleation, where the solid finds itself in an intensely out of equilibrium state due to the optical energy deposited in the electronic subsystem. The network being "cold", the fusion dynamics is determined by the electron-phonon balance, where complete fusion is reached in a few picoseconds. On the other hand, since the ultra-short pulses make it possible to supply an energy which leads to a very high heating rate, temperatures of tens or hundreds of Kelvin per picosecond are easily accessible, which then exceeds the melting temperature and also the static stability limit. Thus, this rapid phase transition is explained by instability of the network due to the excitation of a high density of plasma (electrons-ions).

However, in this case, the network becomes unstable before the phonons heat up [36].

Ultimately, from the moment the transition is ultra-short, the non-thermal physical mechanism is operational. Indeed, such a short melting time cannot be explained by conventional thermal fusion [24] since the ionization of the target is carried out in a much shorter time than the typical time of thermal ablation.

In addition, it has been shown that the size of these particles is due to a mechanical fragmentation mechanism and not from the vapor phase [37].

3.3.3 Plasma formation and surface modification

The last step characterizing the laser-matter interaction is the ejection of plasma of electrons and ions, and of aggregate, accompanied by a possible modification of the ablated surface.

☐ **Plasma formation**

After gaining more laser energy, the electrons become energetic enough to be ejected from the surface of the target. [26] The emission of electrons is due to two phenomena: photoelectric emission and thermionic emission [20]; and it turn out that at high intensities of short duration, photoelectric emission appears to be the dominant mechanism of electron emission [26]. This emission involves the acceleration of the ions in the electrostatic field caused by the separation of charge11created by energetic electrons escaped from the target. Thus, the electromagnetic field due to the charge separation acts on the ions of the target, and at the same time, the ponder motive force due to the laser field in the skin thickness, pushes the electrons deeper into the target, which creates an ion acceleration mechanism in the target. Therefore, a regime of extreme imbalance and ablation of matter takes place. When ionization is complete, the plasma formed in the target's skin layer has a density of free electrons comparable to the density of ions, which is around 1023 cm^{-3} [10].

In ultra-short ablation, the absorption of the laser by the plume can be neglected since this stage is usually generated after the end of the laser pulse [26].

The TTM model does not take into account the formation of the plasma and the plume which comes from the ejection of the target material, therefore, the generation of the resulting plasma is simulated by a hydrodynamic model, which describes the removal of material and the expansion behavior of the plume [26].

☐ **Surface modification**

During irradiation with a femtosecond laser, the ejection of part of the material leaves a crater of different structures (Fig 3.6) [6,23], which forms on the surface of the target such that streaks observed in Figure (2.5) [6].

The formation of these periodic surface nanostructures undoubtedly proves that an induced change in the optical properties of the surface has occurred, where the size and shape of the streaks depends essentially on the shape (wavelength

and number of pulse) of the laser beam and its influence, as well as the dielectric constant of the medium [6,23].

Given the results published in the literature, which are based on the idea that all materials behave in approximately the same way, when they are irradiated by ultra-short pulses at intensities above the threshold of ablation. Under this condition, laser ablation inevitably leads to the generation of nanoparticles of the target material, and this characteristic is of primary interest in nanophysics, and also with a view to possible technological applications for Nano devices [22].
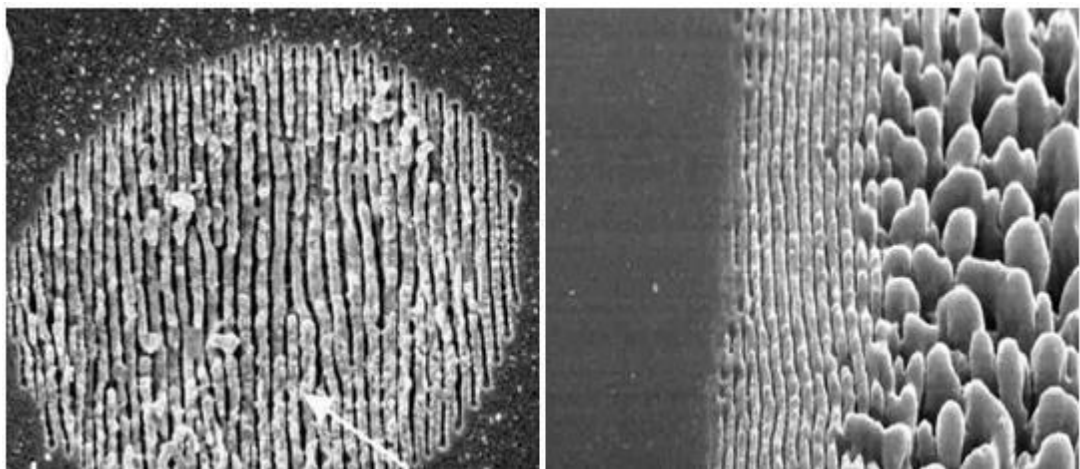
Figure 3.5: Left: Structure formed on a ZnO single crystal with a fluence of 0.48J / cm2; λ = 800nm; τ = 100fs with 50 pulses. Right: Pearl structure in the center of the crater and streaks at the edge, initially only streaks are present.

A closer examination of the irradiated surface using a scanning electron microscope reveals that surfaces of silicon [6] and silicone [23] have been transformed into a forest of peaks of micrometric size. This surface morphology changes after irradiation of silicon and silicone with several hundred laser pulses.
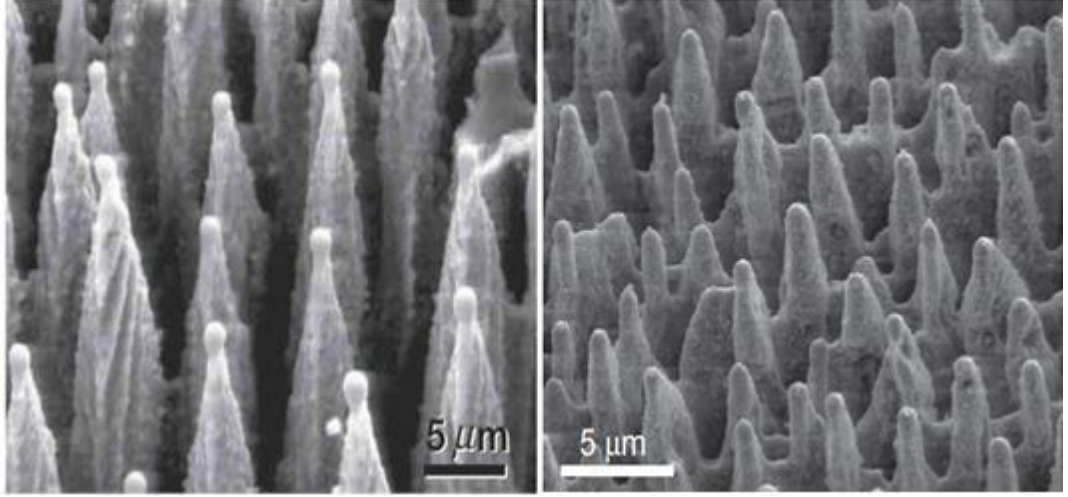
Figure 3.6: Left: conical structure formed on the surface of the irradiated silicon by a hundred pulses of 100fs at a influence of 1J / cm2. Right: structure formed on the surface of silicone, irradiated per 500 pulses of 100fs has a influence of 8J / m^2.

The appearance of craters on the target surface was used as an indicator to determine the heating energy density of the pulse corresponding to the ablation threshold of the surface layer [37].

3.4 System solving

After irradiation with an ultra-short pulse laser, the thermal equilibrium between the electrons is reached in a few femtoseconds, while the heating of the network does not manifest itself until the end of this pulse, which leads to a cooling of the electrons produced. By electron-phonon coupling. This puts us in front of a physical situation of a bath of hot electrons in a network of cold ions, and the two sub-systems supposed to be in thermodynamic equilibrium, can indeed be characterized by their respective temperatures namely T_e and T_i .

As such, heat transfer in metal can be described by a system of two coupled differential equations, each of which obeys the classical law of diffusion.

Fourier heat. The writing of the equations at two temperatures is then given by [20, 22, 25,32]:

$$C_e \frac{\partial T_e}{\partial t} = \vec{\nabla}.\left(k_e \vec{\nabla} T_e\right) - G(T_e - T_i) + S \qquad (3.4a)$$

$$C_i \frac{\partial T_i}{\partial t} = \vec{\nabla}.\left(k_i \vec{\nabla} T_i\right) - G(T_e - T_i) \qquad (3.4b)$$

The terms C_e and C_i represent the electronic heat capacities and the ion network respectively per unit of volume, K_e and K_i are the thermal conductivities of the two subsystems, the term G is the electron-phonon coupling constant, and finally, S is the term heating source, which is actually the laser.

The first equation represents the diffusion of heat between the electrons, and the second equation describes the transfer of heat to the network.

Since the diameter of the laser beam is much greater than the depth of heat penetration, these equations can be simplified to one-dimensional heat transport, eq (3.4) become [32]

$$C_e \frac{\partial T_e}{\partial t} = \frac{\partial}{\partial x}.\left(k_e \frac{\partial T_e}{\partial x}\right) - G(T_e - T_i) + S \qquad (3.5a)$$

$$C_i \frac{\partial T_i}{\partial t} = \frac{\partial}{\partial x}.\left(k_i \frac{\partial T_e}{\partial x}\right) - G(T_e - T_i) \qquad (3.5b)$$

3.4.1 Heat capacity

The calorific capacity C_i (J m^{-3} K^{-1}) of the ion network is in fact only the conventional capacity of the metal. As such, it is practically constant for temperatures above the temperature of Debye. The heat capacity of the electrons is proportional to the temperature of the electrons, with a reduced electronic specific heat coefficient A_e, which depends on the metal considered. It is given by the relation [31, 32, 33]:

$$C_e = A_e T_e \qquad (3.6)$$

This expression is used for electronic temperatures much lower than the Fermi TF temperature:

$$T_F = \frac{E_F}{k_B} \qquad (3.7)$$

The electronic thermal capacity is much lower than the thermal capacity of the network; therefore, the electrons can be heated to very high transient temperatures [17].

3.4.2 Thermal conduction

Like the heat capacity of the network, the thermal conductivity of the Ki ion network is actually only the conventional thermal conductivity of the material. It represents a small portion of the total conductivity, in fact, it is taken at 1% such that [32]:

$$K_i = 0.01 K_S \qquad (3.8)$$

Because.

$$K_i \ll K_S \qquad (3.9)$$

The electronic thermal conductivity cannot be measured explicitly, it is described by an approximation which is sufficient through the expression defined by [25,34]:

$$K_i = K_{oe} \frac{T_e}{T_i} \qquad (3.10)$$

Where K_{oe} represents the thermal conductivity of the material when it is in thermodynamic equilibrium.

For more regions, when the electronic temperatures reach values comparable to that of Fermi, the most suitable expression is [32]:

$$K_i = \chi \frac{(v_e^2 + 0.16)^{1.25}(v_e^2 + 0.44)v_e}{\sqrt{v_e^2 + 0.092}(v_e^2 + \eta v_i)} \qquad (3.11)$$

With $\qquad v_e = \frac{k_b T_e}{\varepsilon_F} \qquad and \qquad v_i = \frac{k_b T_i}{\varepsilon_F}$

3.4.3 The coupling constant

Eq (3.5) are linked by a term which is proportional to the temperature difference between the electrons and the lattice, and to an electron-phonon coupling factor noted G [18].This term designates the energy transferred by electrons to the network per unit of volume of the metal and per unit of time, such as [25,20]:

$$\Delta E = \left[\frac{du}{dt}\right]_{e-ph} = G(T_e - T_i) \quad with \quad G = \frac{\pi^2}{6} \frac{mns^2}{\tau_e T_e} \tag{3.12}$$

Where s is the speed of sound and τ_e the relaxation time of the electrons

In principle, this constant is dependent on the temperature; this dependence disappears for temperatures higher than the Debye temperature [31].

3.4.4 The source term

The term source is the element producing heat by the laser beam. The temporal distribution of this beam is generally like a Gaussian, it represents the density of power brought by a pulse, and is given by [32]:

$$S = 0.94 \frac{1-R}{t_p(\delta + \delta_b)(1 - e^{-d/(\delta+\delta_b)})} J. exp\left[-\frac{x}{(\delta + \delta_b)} - 2.77\left(\frac{t}{t_p}\right)^2\right] \tag{3.13}$$

R being the reflectivity; t_p the width of the laser pulse at mid-height (FWHM); δ and δ_b the respective optical and ballistic ranges; the thickness of the sample and J the influence.

☐**Optical penetration depth**

When a laser pulse is incident on a metal surface, the energy of the laser is absorbed by free electrons in what is called "skin thickness", also called optical depth [33]. It is the depth reached by electromagnetic radiation [34].

☐ **Ballistic penetration depth**

As seen above, the heated electrons will be cooled by two different processes: thermal diffusion by electron-electron collisions, and ballistic movement. In this paragraph, the effect of the ballistic movement of the excited

electrons which make the laser energy penetrate into the depths of the material is reported.

The effect of thermal conduction is modified by adding the ballistic range to the optical depth, in fact, the inclusion of the ballistic effect in the depth distribution of the laser intensity considerably improves the prediction of the model; for the melt influence threshold and the critical electron diffusion length [34].

For transition metals, ballistic transport is not considered, but if it exists, it is in the same range as optical depth [31].

Chapter Four
Numerical Processing

4.1 Introduction

It will be inspired by the two-temperature model as presented by Chowdary et al [32]. Who used it for the interaction of a 100-fs laser pulse with gold in our case it apply the two-temperature model to the study of the interaction of a 290-fs laser pulse with Molybdenum. It use in our work the experimental parameters used by Kotsedi et al [38.39].

4.2 Presentation of the calculation code

Numerical simulation tools occupy a preponderant place in the study of the evolution of quantities and the modeling of the behavior of different physical systems, in our case, because of inhomogeneity of the temperature distribution in the target after irradiation by laser, and because there is a contribution of two temperatures, it chose to carry out this work two software namely: Gambit and Fluent, the first is a mesh generator and the second is a digital solver in finite volume.

4.2.1 Gambit preprocessor

The Gambit tool is a mesh generator that allows you to create your own geometry in 2D and 3D with great precision, it can also provide several types of mesh: structured, non-structure, hybrid in Cartesian, polar, cylindrical and axisymmetric coordinate [40].
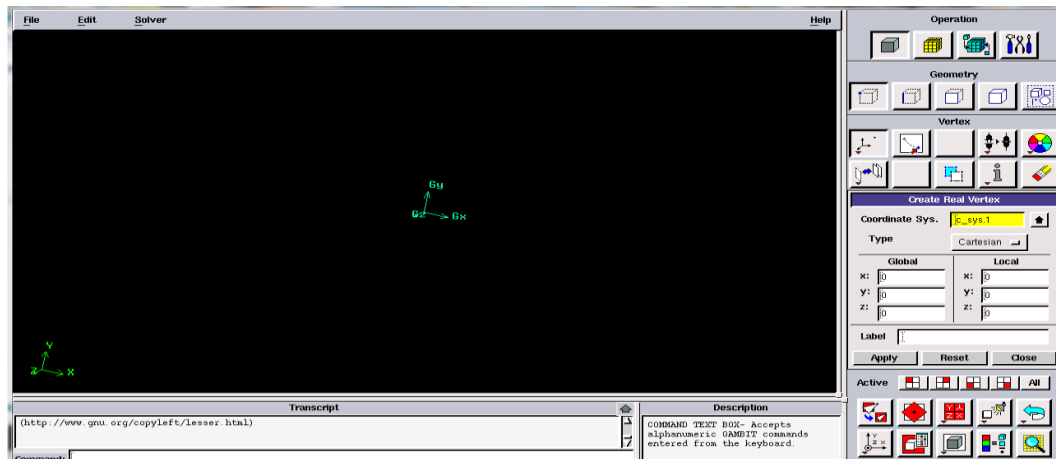
Figure 4.1: Gambit software user interface.

    geometry construction

    geometry mesh

    definition of borders and areas of calculation
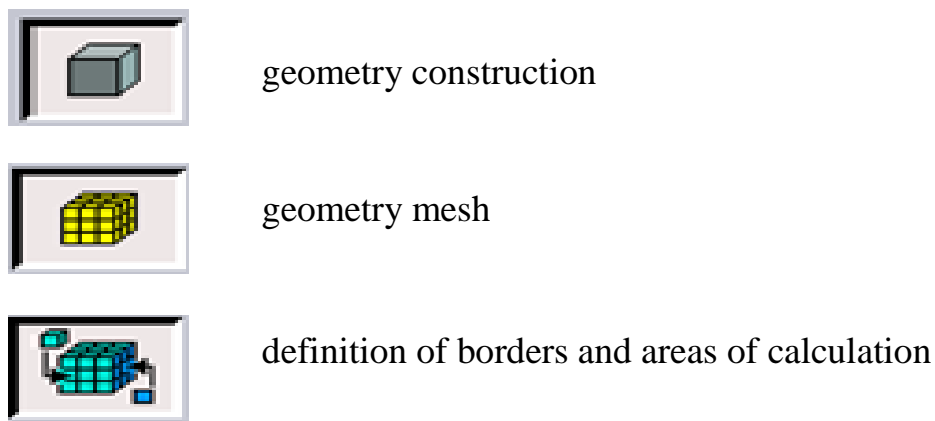
Figure 4.2: Main steps of the mesh software (GAMBIT).

Gambit makes it possible to carry out the following three functions: the construction of the geometry of the problem, the mesh and its verification, and the definition of the borders and fields of computation (initial and boundary conditions). For, generate .msh files used by the Fluent code to solve equations by the finite volume method [40].

4.2.2 Fluent processor

The Fluent software is a digital solver that constitutes a robust simulation tool, used for modeling fluid flows, heat transfers, as well as a multitude of associated phenomena [41].

The Fluent solver is based on the resolution by the finite volume method of the following general conservation equation1 [43] 2:

$$\frac{\partial(\rho\,\phi)}{\partial t} + \overline{\nabla}.(\rho\bar{u}\varphi) = \overline{\nabla}.\left(\Gamma_\phi\overline{\nabla}(\phi)\right) + S_\phi \qquad (4.1)$$

The configuration of models on Fluent is done through a graphical interface; consists of a console, a control panel, a dialog box, and graphical windows. The Fluent console is the main window that controls the program excursion (fig 4.3). It contains a menu bar (file, grid, define, solve) whose elements are arranged to correspond to the typical sequence of actions that you performed in Fluent (ie, from left to right and from top to bottom) [41].


```
FLUENT [2d, pbns, lam]

File   Grid   Define   Solve   Adapt   Surface   Display   Plot   Report   Parallel   Help


     Welcome to Fluent 6.3.26

 |   Copyright 2006 Fluent Inc.
     All Rights Reserved

 Loading "C:\Fluent.Inc\fluent6.3.26\lib\fl_s1119.dmp"
 Done.

 Loading "C:\Users\USER/.cxlayout"
 Done.

 >
```

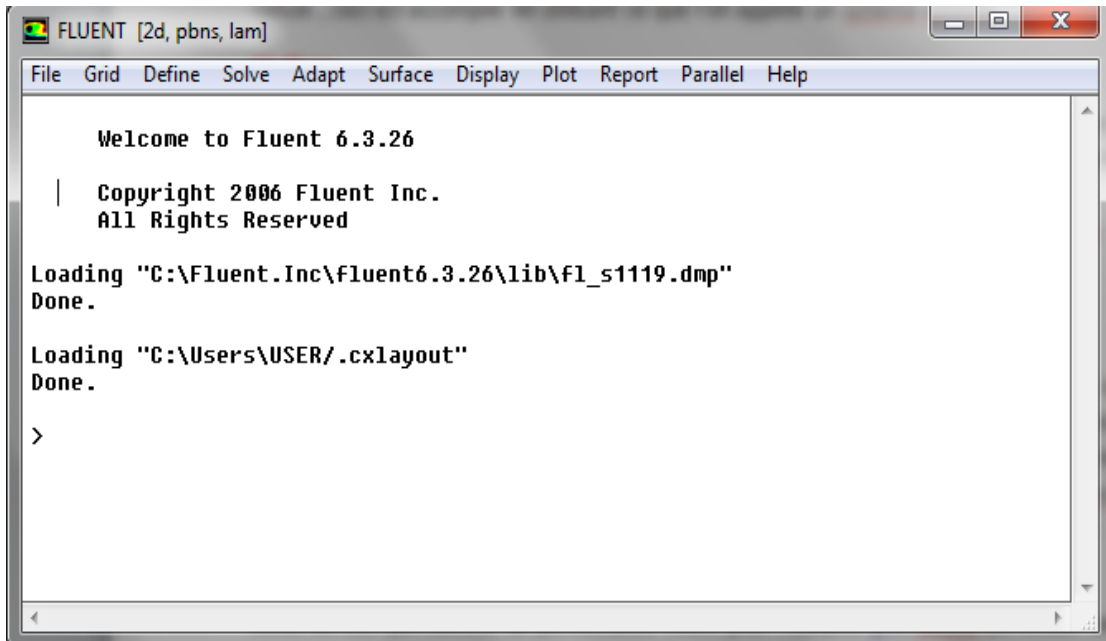**Figure 4.3: The main window of the FLUENT code (the console).**

However, the solver is not intended for the study of ultrashort irradiation heating, Fluent cannot be directly used for the two-temperature model. In order to adapt the solver to the resolution of these coupled differential equations, a code must be developed by the user, and interpreted by the solver, called UDF (User-Defined Function).

☐ **The UDFs**

UDF is user-defined code in the C ++ programming language, which improves the standard characteristics of the code, and extends the capabilities of the solver, so UDFs allow you to customize Fluent for the " adapt to a particular need required in modeling; they can be used in various applications such as: the definition of own boundary conditions, the properties of materials, the adjustment of the values calculated at each iteration, the initialization of a solution, as well as the specification of the parameters of the personalized model such as the source term in the transport equation for a given scheme [42].

☐ **The VOF method**

In Fluent, three different multiphasic Euler-Euler models are available: the mixture model, the Eulerian model, and the Volume Of Fluid (VOF) model [41].

The VOF (Volume Of Fluids) method, known as an interface monitoring method evolving over time, is a technique used for the simulation of interface flows designed for two or more immiscible liquids, it is a multiphasic flow method where a single set of momentum equations is shared by the fluids, and the volume fraction of each of the fluids in each calculation cell is followed throughout the domain, taking into account the voltage of surface, mass transfer and heat between phases [41].

One of the typical applications included in the model is the permanent or transient monitoring of any interface between a liquid and a gas, such as liquid metal and ambient air.

In our case, It assume two regions 'two domains in digital language', the first region represents air and the second represents the target, which explains the hypothesis of using the VOF model.

4.2.3 Discretization of equations by the finite volume method

As It mentioned before, the two-temperature model is described by a system of differential equations with coupled nonlinear partial derivatives, the resolution of this system requires the use of numerical methods, the method chosen for solving these equations is the finite volume method.

In numerical analysis, the finite volume method requires the discretization of the study area, that is to say the subdivision of the study area into elementary volumes called mesh or cells connected together by nodes, all of the cells constitute the mesh.

4.2.4 Initial conditions and boundary conditions

Since the equations represent a non-stationary system, the resolution of this system requires establishing initial conditions, to do this, It has chosen to associate with electrons and ions the same temperature of 300 K which represents the temperature medium ambient.

As for the boundary conditions, it represents the exchange by convection between the external environment and the target studied [25]:

$$K.(\overline{\nabla}T).\vec{n} = H(T_{ext} - T) \tag{4.2}$$

H: Heat exchange coefficient.

4.3 Calculation and Results

4.3.1 Operating conditions

The operating conditions, concerning the laser beam, the sample treated, and the environment are:

☐ **The laser beams**

It is an Nd-YAG laser which emits infrared radiation with a wavelength of 1064 nm. The pulse delivered, with a half-time duration (FWHM) of 290 fs, is focused on the surface of the sample on a spot of 20 μm in diameter. The fluence corresponding to the energy density focused in the focal task is equal to 35 J / m^2.

☐ **The processed sample**

As described by Kotsedi et al. [38.39], the treated material is obtained from the deposition of a thin layer of molybdenum with a thickness of 1 μm on a glass substrate. The deposit is obtained under vacuum at a pressure of 10-7torrs. The thermo-physical properties of molybdenum are given in the table (4.1):

Table (4.1) the thermo-physical properties of molybdenum

Designation	Abbreviation	Value	Unit
Specific heat in solid phase	C_{ps}	516.7	$J\ kg^{-1}\ K^{-1}$
Specific heat in liquid phase	C_{pl}	491.6	$J\ kg^{-1}\ K^{-1}$
Electron – lattice coupling factor	G	13×10^{16}	$Wm^{-3}K^{-1}$
Enthalpy of evaporation at boiling temperature	L_v	6233062	$J\ kg^{-1}$
Enthalpy of fusion	L_f	385300	$J\ kg^{-1}$
Molar weight	M_a	94.95	$kg\ kmol^{-1}$
Infrared reflection coefficient	R	0.189	--
Critical temperature	T_c	13573	K
Melting temperature	T_f	2896	K
Coefficient for electronic thermal conductivity	B_e	122	$J\ m^{-3}K^{-2}$
Radiation penetration depth	δ	35	nm
Fermi energy	E_f	6.77	eV
Solid phase thermal conductivity	k_s	138	$Wm^{-1}K^{-1}$
Thermal conductivity in liquid phase	k_l	71.7	$Wm^{-1}K^{-1}$
Solid state density	ρ_s	10200	$kg\ m^{-3}$
Density in the liquid state	ρ_l	9330	$kg\ m^{-3}$

☐ **The environment**

In our modeling, It consider an environment under normal conditions of pressure (101325 Pa) and temperature (300 K).

4.3.2 Geometry of the problem

The modeling begins with the determination of the geometry of the domain, its mesh, and the reservation of the boundary conditions. To prepare the geometry by using the Gambit preprocessor, associated with the digital fluid dynamics software Ansys / Fluent CFD [40,41]. Our geometry must include a sub-domain

to represent the ambient air, and another sub-domain to represent the material (Molybdenum).

The figs (4.4) represent the area of calculation including the air and the treated material. The dimensions of the calculation field are x_{min} = -50µm, x_{max} = 50µm, y_{min} = -50µm, y_{max} = 50µm, z_{min} = -1µm, z_{max} = 1µm.

The laser beam is focused on the air-material interface (dark gray) on a task of 20 µm in diameter, having as its center the origin of the reference (0xyz)
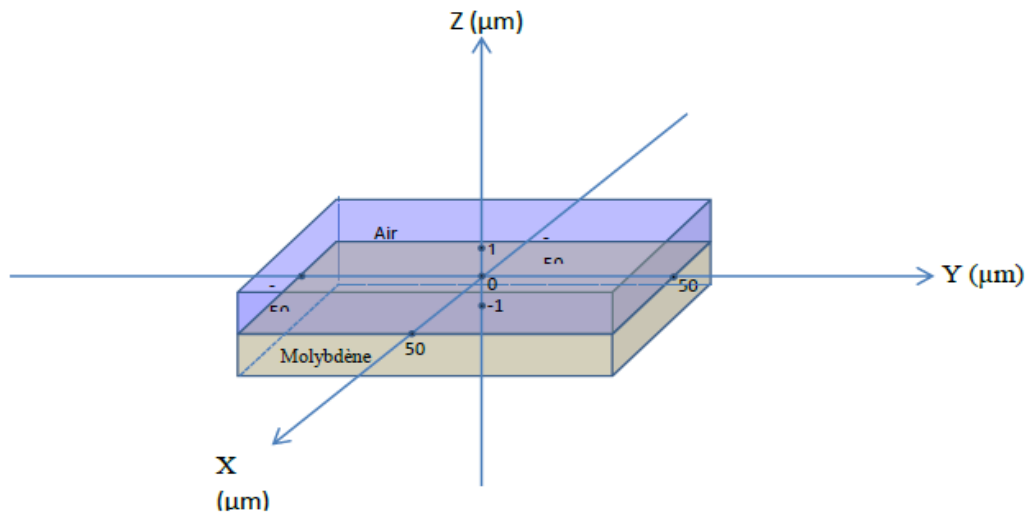

Figure (4.4): Dimensions of the calculation domain.

The mesh of the computational domain includes the mesh of faces and volumes. The computing domain includes 154,500 faces located on the boundaries of the domain, 50,000 cells contained in the two volumes containing the air and the material, with 25,000 cells for each sub-domain. Finally, the number of nodes in the computation domain is 54,621 nodes.

The mesh used is structured; it is composed of quadrilaterals on the faces and hexahedral elements in the two sub-volumes. The figure (4.5-a) shows the mesh used in our simulations. The mesh being very refined, the figure seems uniform, and does not show the details of the mesh, making that the meshes are not visible. To have an idea on the mesh used, the fig (4.5-b) represent an enlargement of a region located on a corner of the field of computation.
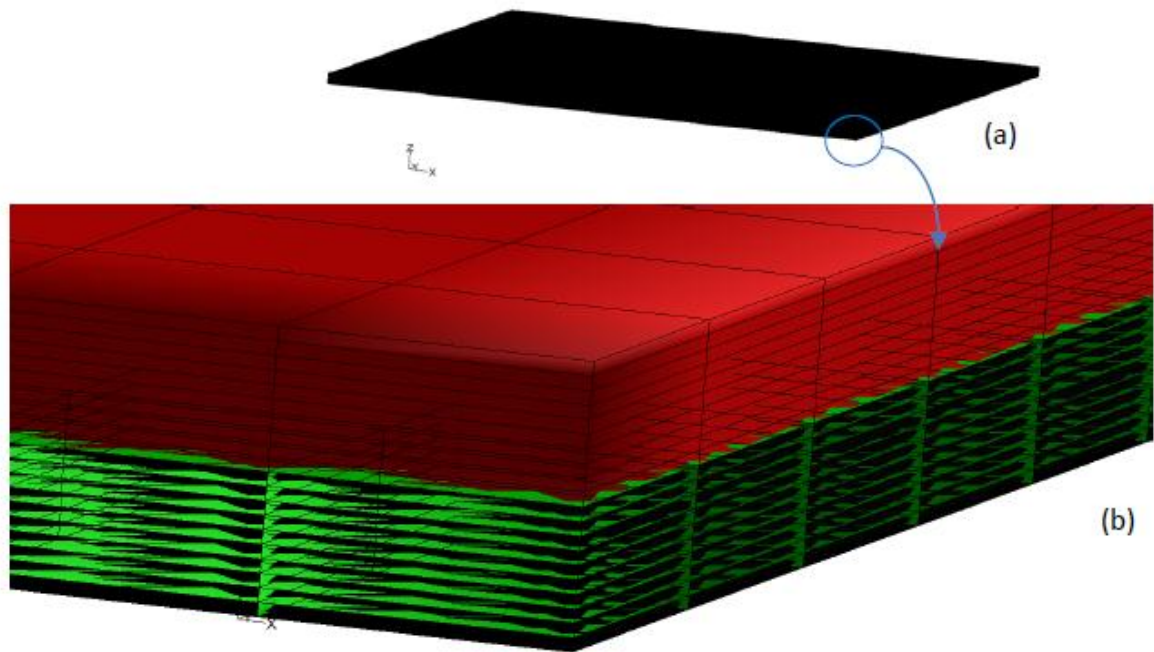
Figure (4.5): Meshing of the calculation field, with enlargement showing the two sub-domains: air in red, and material in green.

The enlargement of the fig (4.5) makes it possible to distinguish the mesh located on the thickness of the material in the direction Z, in the negative direction, and could count ten meshes along the thickness of 1μm, which allows to subdivide the thickness of the meshes having a dimension of 100 nm along Z. The boundary conditions which are applied on the domain are:

- The condition called "Heat Flux" where the temperature gradient is canceled on the walls of the material, which allows to maintain the continuity of the heat transfer.

- The condition called 'Outlet Pressure' on the air walls, which allows continuity of atmospheric conditions beyond the field of calculation.

One considers as initial condition a temperature of 300 K in all the field of computation.

4.3.3 Application of the laser pulse

The application of the TTM model implies that it is the free and bound electrons which constitute the electronic gas, which will absorb the laser energy while the metal ions of the network will not feel any effect because of the slowness of the response time to such irradiation.

The fig (4.6) give the evolution of the temperature field in the electronic gas observe a rapid rise during the first hundred femtoseconds, then a moderate rise up to 290 fs, where an extremely high temperature of the order of 8000 K is reached.
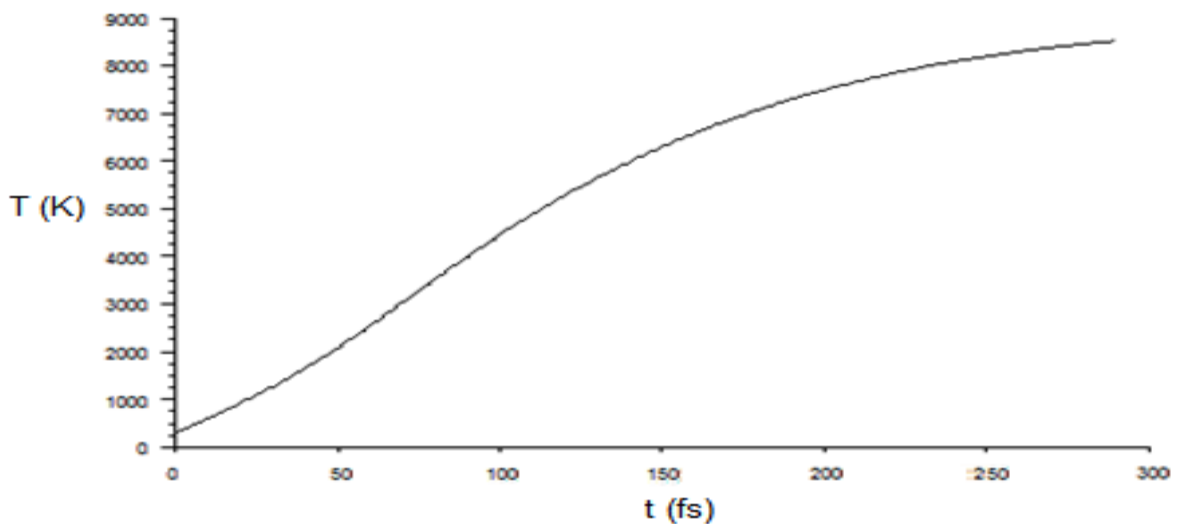

Figure (4.6) the evolution of the temperature field in the electronic gas.

The fact of reaching a temperature of 8000 K by the electronic gas in such a short period of time does not imply that the material is at the electronic temperature, thus, the material will not begin to receive energy until through the exchange with electronic gas, well after the laser pulse has ended.

The fig (4.7) shows us the temperature field in the irradiated region containing in the focal spot of the laser beam which is established at 20 μm in diameter. It is noted from the observed temperature gradient that the surface of the sample rapidly changes from an extremely high temperature (8000 K) to a temperature close to room temperature. The treated region is thus extremely localized, which constitutes one of the advantages of the use of ultrafast lasers in micro and nanotechnology applications.
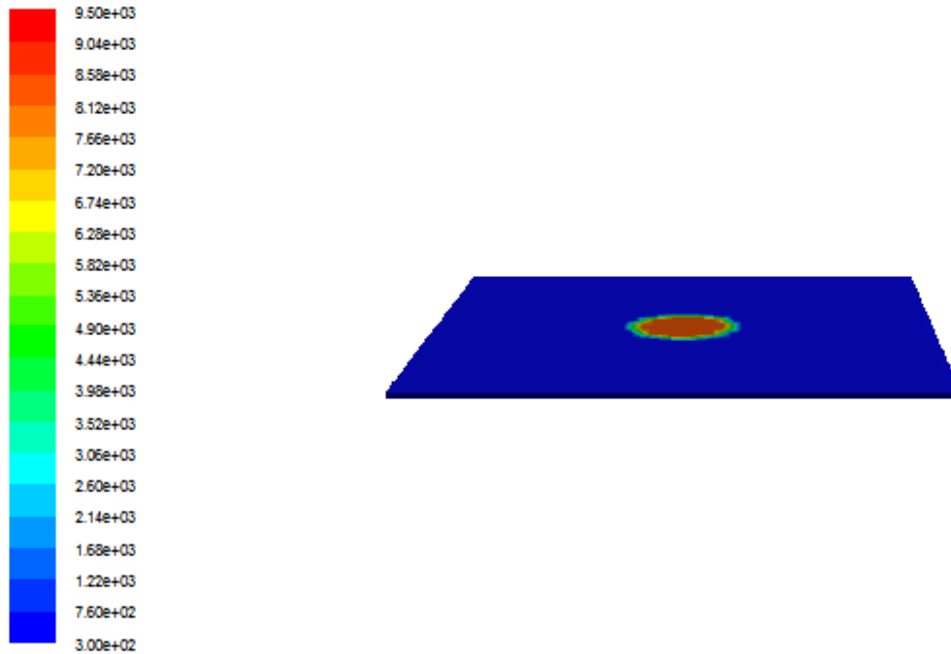
40

Figure 4.7: Distribution of the temperature field on the Molybdenum-air interface at the end of the 290-fs laser pulse for a focal task of the laser beam of 20μm in diameter and a laser influence of 35J / m^2

4.3.4 After switching off the laser pulse

After the laser pulse goes out, the relaxation phenomenon takes effect. The electrons having absorbed the electromagnetic energy during the duration of the pulse will redistribute the accumulated energy to the ions of the network, for a relatively long duration, of the order of several hundreds of picoseconds.

This redistribution is accompanied, as seen in fig (4.8), obtained by the implementation of the second equation (eq 3.4) of the TTM model for the network, of a decrease in temperature for a duration of more than 1000 times the duration of the laser pulse.

It is only in this time interval that the thermal effects are "felt" by the material, through its heat capacity, its density, and its thermal conductivity.

As shown in Fig (4.8), the material can, during relaxation and redistribution of energy, go through the vapor and liquid phases, in a time of the order of magnitude of a few picoseconds. This makes it possible to envisage so-called

thermal treatments, which make it possible to obtain craters or furrows of very high qualities from the point of view of the formation of burrs, which are relatively reduced by this process.
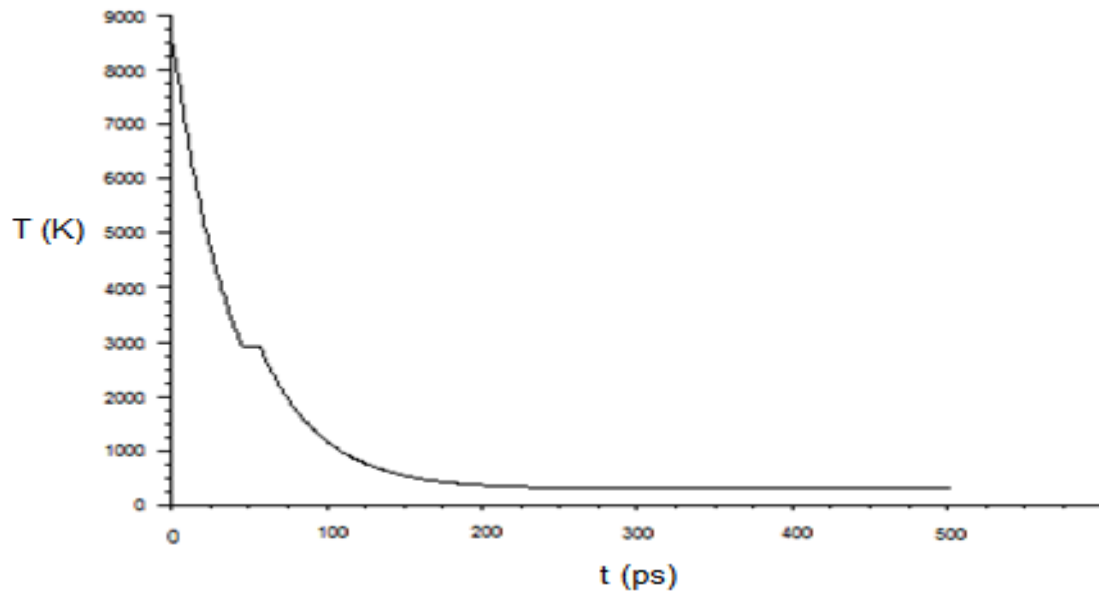

Figure 4.8: Temperature field after switching off the laser pulse (relaxation).

Chapter Five

Conclusion and Recommendation

5.1 Introduction

The study generally presents the mechanism of ablation of metals by ultrafast laser pulses; the main part was devoted to understanding a particularly interesting case: femtosecond pulse laser irradiation.

In an extremely short duration, of the order of a hundred femtoseconds (1fs = 10^{-15}s) the material sees the energy deposited over a length comparable to the thickness of optical penetration which is of the order of ten nanometers for several metals. It is considered on this timescale that the material treated is divided into two subsystems in the case of metals: the ionic network composing most of the material, and the electronic gas composed of free or bound electrons. On the time scales of a laser pulse lasting a few hundred femtoseconds, only the electrons respond to the electromagnetic stress and it is the electrons that absorb the laser energy while the ions in the network have no time to feel the electromagnetic shock and remain undisturbed. These are the electrons that redistribute in the network the energy gained well after the end of the laser pulse.

5.2 Conclusions

In this research, generally present the mechanism of ablation of metals by ultrafast laser pulses. The main part was devoted to understanding a particularly interesting case: femtosecond pulse laser irradiation.

The heating processes as well as the main characteristics of material transformation, in particular the rapid creation of steam and the formations of the plasma phase as well as the surface structure were introduced.

The aspect characterizing the femtosecond metal-laser interaction is the fact that large quantities of optical energy can be deposited in the metal in a much shorter time than the time necessary for the thermalization of the energy, which implies a very fast tearing of material, so that the coupling rate with the network in this pulse regime is very low. In other words, the propagation of heat in the material is negligible. Such an infinitely short interaction time of vaporization of the material cannot be considered by a conventional thermal fusion, which makes it possible to admit that the phenomenon is non-thermal, or thermal.

A two-temperature model based on the Fourier heat transfer equation describes femtosecond ablation heating. This model consists of two parabolic differential equations coupled by the exchange term between the two subsystems, namely the electron gas and the ion network.

The ultra-rapid heating mechanisms in metallic material have been studied by an approach based on numerical simulation, where the study of ultra-short pulse heating has been carried out on a Molybdenum slide.

The work carried out consists in the construction of a geometry representing the domain of computation, thanks to the Gambit preprocessor, then to solve the equations coupled by the fluent processor. The results obtained concerning the distribution of the temperature field show a conformity with those obtained by o there authors.

The applications that can be envisage with a laser with femtosecond pulses fired at a given frequency (a few MHz) open the way to nonmetric structuring which can be applies to advanced techniques for the exploitation of solar energy for example.

The absence of the liquid phase in the femtosecond ablation, allows us a better control during the drilling process, this opens the opportunity to study ablation with lasers beyond the femtosecond in particular with the implementation work of attosecond lasers.

This study could be a prelude to a more complete investigation, which would concern other applications of femtosecond laser pulses in   the field of microfluidics, MEMs, etc.

5.3 Future Work

 I recommend developing an interaction mechanism between ultra-short pulse laser and some materials

Reference

[1] SOVEJA, Adriana-Florina. Modeling of the texturing process by laser beam: Experimental and digital approaches. Doctoral thesis, U. Bourgogne, "Politehnica" Timisoara (2007)

[2] M. von Allmen. Laser drilling velocity in metals. Applied physics. flight. 47, no.12, December 1976.

[3] F. Barthélémy, P. Christmann. 2010 world panorama of the molybdenum market. Final report. BRGM / RP-60204-FR, 59 p., 14 fig., 5 tabl. 2011.

[4] Jerome Kasparian, Ultrashort pulse power lasers. Futura-Sciences, 25/2/2008. Available at: http://www.futura-sciences.com/magazines/matiere/ infos/dossiers/d/physique-laserspuissance-impulsions-ultracourtes-764/page/2/

[5] DI MAIO, Yoan. Study of the laser-matter interaction in ultra-short pulse regime: Application to micromachining of materials intended for sensors. Doctoral thesis, U. Jean Monnet Saint-Étienne (2013)

[6] DJOUDER, Madjid. Modeling of the formation of nanostructures obtained by laser ablation in femtosecond regime. Doctoral thesis, U. Mouloud Mammeri Tizi-Ouzou (2012)

[7] Jerôme Kasparian. Ultrashort pulse power lasers. Futura-Sciences, P 1-12, 2008. Available in PDF format at: http://www.futurasciences.com/magazines/matiere/infos/dossiers/ d/ physique-laserspuissance-impulsions ultracourtes-764 /

[8] Matthew S. Brown, Craig B. Arnold. Fundamentals of Laser-Material Interaction and Application to Multiscale Surface Modification, chapter 4. Springer-Verlag Berlin Heidelberg, P. 91-120, 2010.

[9] Peter Schaaf. Laser nitriding of metals. Progress in Materials Science, 47, P. 1-161, 2002.

[10] E. G. Gamaly, A. V. Rode, V. T. Tikhonchuk, B. Luther-Davies. Ablation of solids by femtosecond lasers: ablation mechanism and ablation thresholds for metals and dielectrics. Phys. Rev. A, January 2001.

[11] C. Kittel, solid state physics, Dunod (1998)

[12] M. Fourier. Dissertation on the propagation of heat in solid bodies. New Science Bulletin by the Société philomathique de Paris 6, 112_116, 1808. Available at: http://pagespersorange.fr/alta.mathematica/fourier1807.html.17

[13] AMIN CHALHOUB, Eliane. Study of thermophysical processes in laser-matter nanosecond interaction regime by rapid pyro-reflectometry. Doctoral thesis, U. Orléans (2010)

[14] Lonnie Lucas, Jim Zhang, Femtosecond laser micromachining: A back-to-basics primer. Applied Energetics, January 2012.

[15] J.-L. Dumas. Interaction of a laser beam with a metallic target - First part Study of the heating and vaporization of the target. Journal of Applied Physics, 5 (6), P.795-809, 1970.

[16] Guillaume Petite. Fundamental mechanisms of femtosecond laser ablation in "intermediate flow". Irradiated Solids Laboratory, UMR 7642 CEA / DSM, CNRS / SPM and Ecole polytechnique F-91128, Palaiseau. Available on :

http://arxiv.org/ftp/cond mat / papers / 0502 / 0502132.pdf

[17] B.N. Chichkov, C. Momma, S. Nolte, F. von Alvensleben, A. Tünnermann. Femtosecond, picosecond and nanosecond laser ablation of solids. Applied physics A, 63, P. 109-115, 1996.

[18] T. Niu, Louisiana Tech University. A Hyperbolic Two-step Model Based Finite Difference Method for Studying Thermal Deformation in a Micro Thin Film Heated by Ultrashort-pulsed Lasers. Louisiana Tech University, 9780549261131, ProQuest, 2007, 143 p.

[19] S. I. Anisimov. Effect of very short laser pulses on absorbing substances. Soviet physics JETP, volume 31, n ° 1, P. 337-340, July 1970.

[20] S. I. Anisimov, B. L. Kapeliovich, T. L. Perel'man. Electron emission from metal surfaces exposed to ultrashort laser pulse. Soviet physics JETP, vol. 39, n ° 2, P. 776-781, August 1974.

[21] T. Q. Qiu, C. L. Tien. Heat transfer mechanisms during short-pulse laser heating of metals. ASME J. Heat Transfer, vol. 115, n ° 4, P. 835-841, November 1993.

[22] S. Amorus, B. Bruzzese, X. Wang, N N Nedialkov, P. A. Atanasov. Femtosecond laser ablation of nickel in vacuum. Applied physics D, 40, P. 331-340, 2007.

[23] TULL, Brian Robert. Femtosecond Laser Ablation of Silicon: Nanoparticles, Doping and Photovoltaics. Doctoral thesis, U. Harvard (2007)

[24] D. Von der Linde, K. Sokolowski-Tinten, J. Bialkowski. Laser – solid interaction in the femtosecond time regime. Applied Surface Science, 109/110, P. 1-10, 1997.

[25] VALETTE, Stéphane. Thermal effects due to the laser-matter interaction in metals in femtosecond regime. Doctoral thesis, U. Jean Monnet, Mines Saint-Etienne (2003)

[26] Xin Zhao, Yung C Shin. A two-dimensional comprehensive hydrodynamic model for femtosecond laser pulse interaction with metals. Applied physics D, 45, 105201, P. 12, 2012.

[27] Roman V. Dyukin, George A. Martsinovskiy, Olga N. Sergaeva, Galina D. Shandybina, Vera V. Svirina, Eugeny B. Yakovlev. Interaction of Femtosecond Laser Pulses with Solids: Electron / Phonon / Plasmon Dynamics, Chapter 7. licensee InTech, 2012.

[28] Koji Sugioka, Ya Cheng. Femtosecond laser processing for optofluidic fabrication. Critical review, 2012.

[29] G. Mainfray, C. Manus. Multiphotonic Transitions. Journal de Physique Colloques, 39 (C1), P.C1-1-C1-16, 1978.

[30] M. Casalino, Near-Infrared Sub-Bandgap All-Silicon Photodetectors. International Journal of Optics and Applications, Vol. 2, n ° 1, pp. 1-16, 2012.

[31] J. Hohlfeld, S. –S. Wellershoff, J. Güdde, U. Conrad, V. Jähnke, E. Matthias. Electron and lattice dynamics following optical excitation of metals. Chemical Physics, 251, P. 237-258. 2000.

[32] I. H. Chowdhury, X. Xu. Heat Transfer in Femtosecond Laser Processing of Metal. Numerical Heat Transfer, Part A, 44, P. 219-232, 2003.

[33] Feng Chen, Guangqing Du, Qing Yang, Jinhai Si, Hun Hou. Ultrafast Heating Characteristics in Multi-Layer Metal Film Assembly Under Femtosecond Laser Pulses Irradiation, Two Phase Flow, Phase Change and Numerical Modeling, Dr. Amimul Ahsan (Ed.), ISBN: 978-953-307-584-6, In Tech, 2011.

[34] J. K. Chen, J. E. Beraun. Numerical study of ultrashort laser pulse interactions with metal films. Numerical heat transfer, part A, 40: P. 1-20, 2001.

[35] Li Yang, Ching-Yue Wang, Wei Yang. Numerical Simulation and Analysis on 3D Temperature Field of the Metal Ablated with Femtosecond Pulse Laser. Journal of Physics: Conference Series, 276, 012032, P. 1-5, 2011.

[36] B. Rethfeld, K. Sokolowski-Tinten, D. von der Linde, S. I. Anisimov. Ultrafast thermal melting of laser-excited solids by homogeneous nucleation. Physical Review B, volume 65, 092103, 2002.

[37] M. B. Agranat, S. I. Anisimov, S. I. Ashitkov, A. V. Ovchinnikov, P. S. Kondratenko, D. S. Sitnikov, V. E. Fortov. On the Mechanism of the Absorption of Femtosecond Laser Pulses in the Melting and Ablation of Si and GaAs. JETP Letters, vol. 83, n ° 11, P. 501-504, 2006.

[38] L. Kotsedi, Z. Y. Nuru, P. Mthunzi, T. F. G. Muller, S. M. Eaton, B. Julies, E. Manikandan, R. Ramponi, M. Maaza. Femtosecond laser surface structuring and oxidation of chromium thin coatings: Black chromium. Applied Surface Science, 321, P. 560-565, 2014.

[39] L. Kotsedi, P. Mthunzi, S. M. Eaton, Z. Y. Nuru, P. Sechoghela, N. Mongwaketsi, R. Ramponi, M. Maaza.Femtosecond laser surface structuring of molybdenum thin films, 1993.

[40] www.ansys.com

[41] RANARIJAONA, Zo Alain.Study of deviations from thermal equilibrium in arc plasmas.Doctoral thesis, U. Toulouse (2011).